

INFLUENCE OF FIBRE REINFORCEMENT ON THE DEVELOPMENT OF INTERFACE MORPHOLOGY DURING COMPOSITE INJECTION OVERMOULDING

R. MacLennan¹, M. A. Aravand^{1,2*}

¹ School of Mechanical and Aerospace Engineering, Queen's University Belfast, Belfast, United Kingdom,

² Northern Ireland Advanced Composites and Engineering (NIACE) Centre, Belfast, United Kingdom

* Corresponding author (m.aravand@qub.ac.uk)

Keywords: Composite injection overmoulding, Interface, Morphology, Simulation, Micro-scale

ABSTRACT

Composite injection overmoulding offers complex composite structures to be manufactured rapidly and with unrivalled dimensional accuracy. However, understanding the formation of the interface between the injected melt and the substrate remains a challenge and is a multi-scale process. Although there have been efforts to understand the process of interface formation the majority of the work on the subject thus far has not focussed on the micro-scale. In this work, the role of fibre reinforcement is investigated through experimental and simulation means. Following overmoulding of glass and carbon-reinforced laminates the interface is examined, and lap-shear coupons are tested. An accompanying computational fluid dynamics (CFD) simulation of the interface formation process has been developed.

1 INTRODUCTION

The composite injection overmoulding process has the potential to offer considerable benefits in the manufacture of composite structures. During the process, features are injection moulded directly onto a thermoplastic composite which is contained within a mould tool to produce a new structure. During injection and consolidation, interdiffusion between molecules of the injected polymer and the substrate matrix leads to the development of bonds and a new, complete structure is produced. The main benefits offered are a considerable reduction in labour as complex features may be produced with rapid cycle times and improved dimensional accuracy [1, 2]. Furthermore, the additional strength-to-weight ratio of continuous fibre composites is realised and the structure is not weakened through the use of fasteners or adhesive bonding.

One of the challenges facing the implementation of this process, however, is that the interface between the injected polymer and substrate is a critical region which is affected by processing variables such as temperature (of both the injected material and substrate) as well as material selection (which includes both polymer and fibre content within both the injected melt and substrate) which can influence the development of polymer bonds through means of altering the thermal behaviour at the interface and through compatibility [3, 4].

At present, there have been studies to understand the development of bonds between the injected melt and substrate. Current approaches have been through the implementation of analytical models to estimate local bond strength due to interface 'healing' as well as through molecular dynamics simulation [5-10]. These have been applied at the macro and molecular scales, respectively. Due to their implemented scales, neither of these approaches considers the change in interface morphology because of processing which occurs at the microscale. It has been observed that processing may result in an interface that is not comparable to the initial conditions [11, 12]. Furthermore, the influence of fibres on interface morphology may not be easily implemented. The approach in this work is to use a multi-phase computational fluid dynamics model to investigate the formation of the interface morphology during the composite overmoulding to understand the changes in interface morphology with respect to the variation in fibre reinforcement of the substrate.

2 METHODOLOGY

In the following work, the interface formation process has been investigated through experimental means and the use of simulation tools. For the experimental work specimens have been produced through overmoulding, allowing for their microstructure to be investigated. To further understand the development of the interface microstructure the interface formation process has also been simulated. Since the interface formation occurs at multiple scales, a multi-scale approach has been implemented to capture key processes at the micro-scale and macro-scale.

2.1 Preparation of samples

Rectangular coupons were prepared from Toray Cetex TC1100 woven polyphenylene sulfide (PPS) composite containing carbon (T300) and glass (E-glass) fibres of comparable fibre volume fraction (~50%). After subsequent surface preparation coupons were overmoulded with discontinuous carbon filled (30%) polyetheretherketone (PEEK) Evonik Vestakeep 2000 CF30.

Following the successful overmoulding of the samples, lap-shear coupons were manufactured from the specimens.

2.2 Composite injection overmoulding simulation

The above overmoulding process has been simulated within Autodesk Moldflow (v2021.1). The insert has been modelled as a solid region specifying the thermal properties of the substrate. The relevant material and processing settings were selected such that they matched the materials used in the experiment.

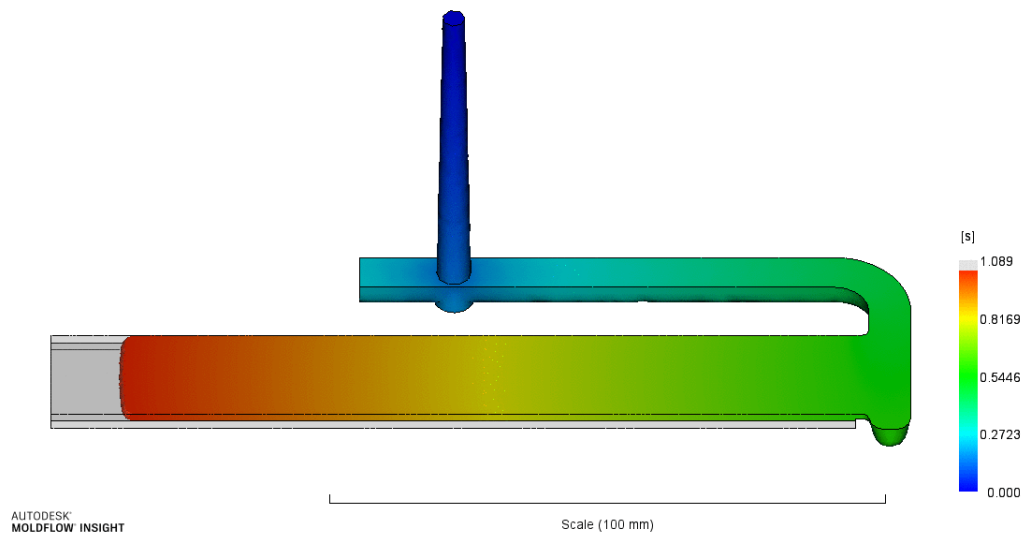


Figure 1: Macro-scale flow simulation of coupon overmoulded, performed within Autodesk Moldflow.

From the above macro-scale simulation, relevant boundary conditions could be obtained for the micro-scale interface formation simulation, notably injection velocity and temperature.

2.3 Simulation of interface formation

The interface formation was simulated through the finite volume method computational fluid dynamics package Ansys Fluent (v2020 R2). The key processes captured include the melting of the insert matrix and the subsequent fluid interaction of the injected phase. For capturing the interaction of phases the Volume of Fluid (VoF) model is implemented. In the VoF model, mass continuity is solved for each phase, denoted by q .

$$\frac{1}{\rho_q} \left[\frac{\delta}{\delta t} (\alpha_q \rho_q) + \nabla \cdot (\alpha_q \rho_q \vec{v}_q) \right] = 0 \quad (1)$$

Where α_q is the volume fraction of phase q . Volume-averaged properties are calculated by the following expression, in the example of the calculation of density:

$$\rho = \sum_{q=1}^n \alpha_q \rho_q \quad (2)$$

Volume-averaged properties calculated through the above are then implemented in the following momentum conservation on a shared field for all phases.

$$\frac{\delta}{\delta t} (\rho \vec{v}) + \nabla \cdot (\rho \vec{v} \vec{v}) = -\nabla p + \nabla \cdot [\mu (\nabla \vec{v} + \nabla \vec{v}^T)] \quad (3)$$

Energy conservation is also calculated on a shared field using volume-averaged properties:

$$\frac{\delta}{\delta t} (\rho E) + \nabla \cdot (\vec{v} (\rho E + p)) = \nabla \cdot (k \nabla T + (\vec{\tau} \cdot \vec{v})) \quad (4)$$

Boundary conditions implemented from the Moldflow simulation are applied to the following 2D fluid domain shown in Figure 2. At initialization of the solution, it is assumed that the small section of fluid included within the domain is initially in a state of perfect contact between the injected melt of the injected material. It is assumed that initially there is a flat separation between the injected melt and the substrate.

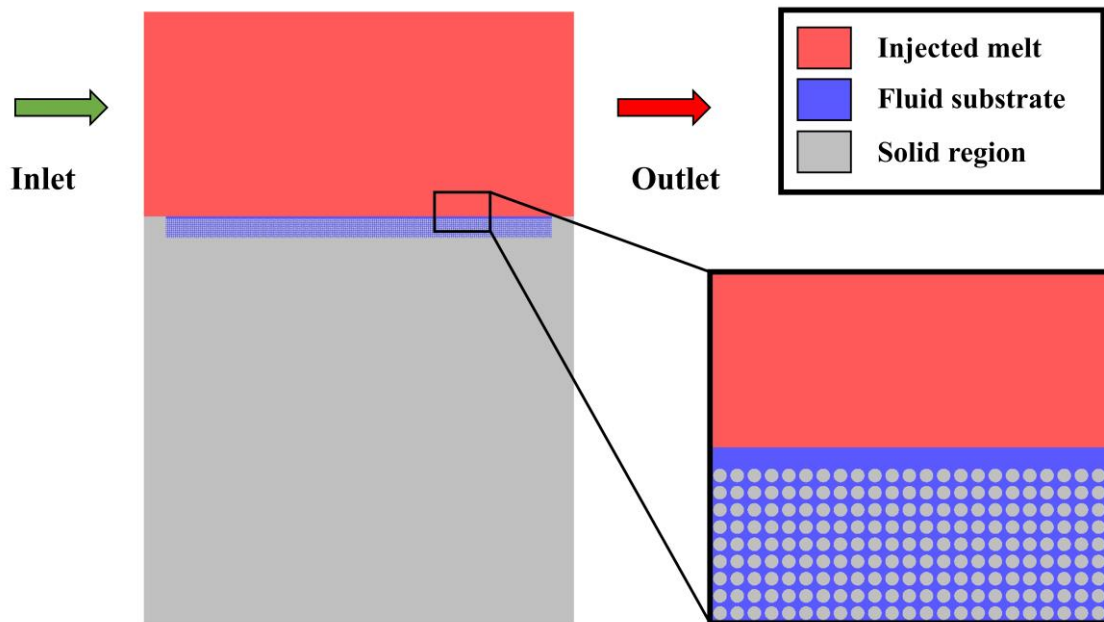


Figure 2: Image of the micro-scale simulation domain showing the regions patched at the initial condition of the simulation and detail of the fibre reinforcement at the interface.

A no-slip condition is assumed at the fibre boundary and the material properties of the carbon fibre region have been obtained from manufacturer specifications. Fibre regions are considered to be constrained from motion and it is assumed that they are not displaced by fluid flow. Energy transfer is active in the solid region and a coupled thermal boundary is active between the fluid and solid regions. Non-Newtonian polymer viscosity is implemented through a modified generalized Newtonian model

incorporating the effects of solidification. The approach of Kattinger, et al. [13] was used which modifies the Cross-WLF to include solidification behaviour:

$$\eta = \frac{\eta_0}{\left[1 + \left(\frac{\eta_0 \dot{\gamma}}{\tau}\right)^{1-n}\right]} \quad (5)$$

Where, η is the polymer viscosity (Pa s), η_0 is the zero-shear viscosity, $\dot{\gamma}$ is the shear rate (1/s), τ is the critical stress upon transition to shear-thinning and n is the power-law index. To impose the solidification behaviour, a sharp rise in viscosity is implemented using a hyperbolic tangent function:

$$MF = \left[\frac{\tanh(TS(T-T_m))+1}{2}\right]^{MS} \quad (6)$$

Where MF is the calculated melt fraction, T is the local temperature, T_m is the melting point of the polymer. TS and MS are simulation parameters that may be modified to give the desired solidification behaviour.

While $T > T_m$, the variation in zero-shear viscosity due to temperature is provided by the WLF equation in the usual manner:

$$\eta_0 = D_1 \exp\left[\frac{-A_1(T - D_2)}{A_2 + (T - D_2)}\right] \quad (7)$$

Where η_0 is the zero-shear viscosity and A_1 , A_2 , D_1 , and D_2 are data-fitting parameters. For $T < T_m$, the following correction is made to the viscosity model:

$$\eta_0 = D_1 \exp\left[(1 - MF) \cdot \left(\frac{-A_1(T_m - D_2)}{A_2 + (T_m - D_2)}\right) + MF \cdot \left(\frac{-A_1(T - D_2)}{A_2 + (T - D_2)}\right)\right] \quad (8)$$

3 RESULTS AND DISCUSSION

Investigation of the interfaces formed following overmoulding of the carbon and glass laminates yielded interface morphologies of similar configuration. The separation between the injected melt at the substrate is variable and chaotic and the height of observed features varies with streamwise locations. Larger scale features are present closer to the inlet of the coupon due to the increased contact time of the substrate with advancing melt flow.

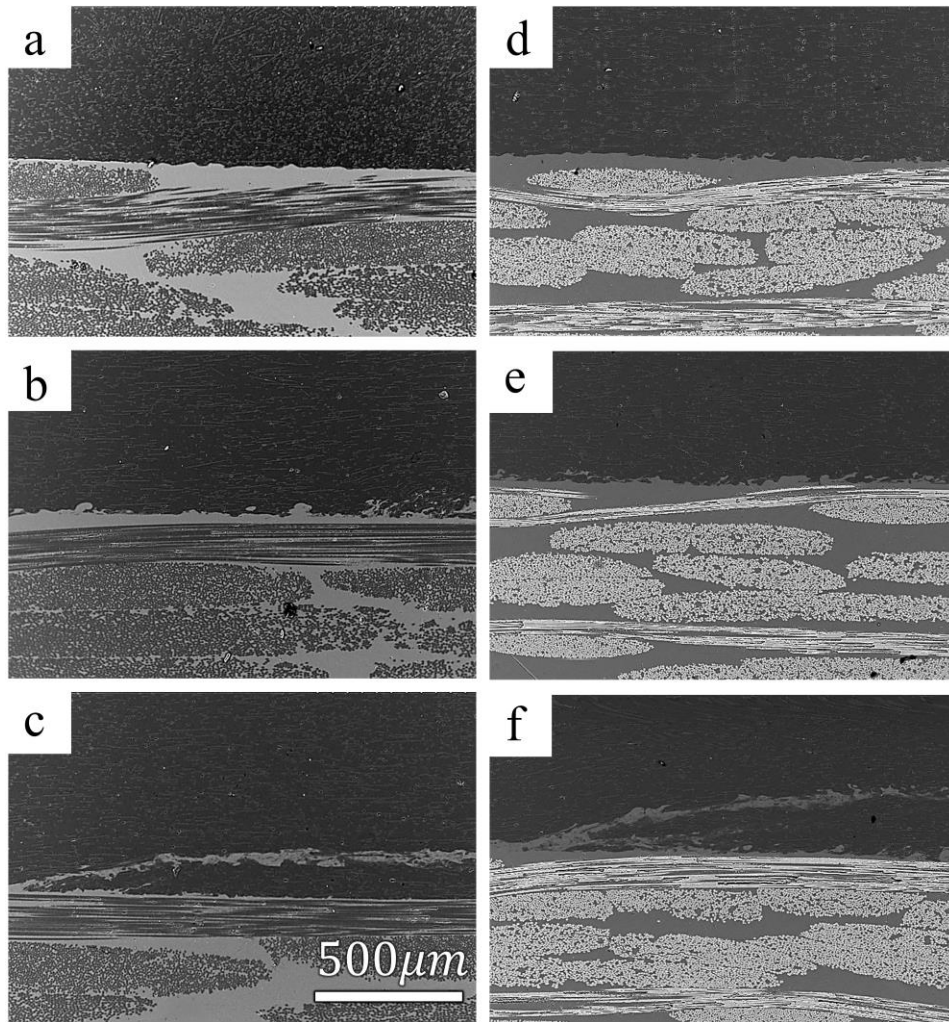


Figure 3: Comparison of interface morphology at locations within an overmoulded sample following injection of CF-filled PEEK over woven PPS laminate with increasing contact time: Locations farthest downstream of, at mid-point, and within proximity to the injection location for a carbon-reinforced woven (a, b, c) and glass-reinforced (d, e, f) laminate.

The irregular features present at the interface may be explained by the interaction of the injected melt with the polymer at the surface of the substrate. An image of the simulation output showing the development of the interface morphology is shown in Figure 4. Following the melting of the surface substrate, the development of features at the interface features is possible due to the presence of velocity-shear between the injected melt and substrate fluids. This causes the interface features to increase in size over time.

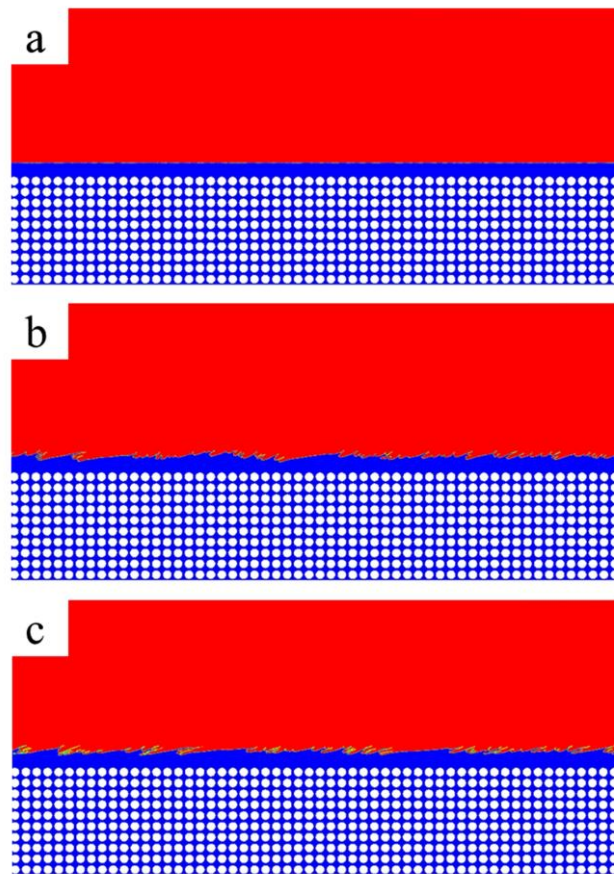


Figure 4: Contour of phases during simulation of interface formation during injection of CF-filled PEEK (red) over carbon-reinforced PPS (blue) laminate. Shown at times $t = 0s, 0.001s$ and $0.01s$, respectively.

A comparison of interface thermal history for the carbon and glass simulations reveals that for the same initial conditions, process settings and fibre geometry selected glass fibres offer favourable conditions for the development of interface strength: an increased interface temperature is recorded throughout the process simulation. The temperature history recorded at locations near the interface also shows consistently higher temperatures for the glass-reinforced system. This indicates that there is greater diffusion of energy from the injected melt in the case of the carbon-reinforced laminate due to increased thermal conductivity. However, this is accompanied by a greater rate of diffusion through the laminate. The increased interface temperature of the glass-fibre reinforced system is thus explained by the reduced thermal conductivity of the glass fibres.

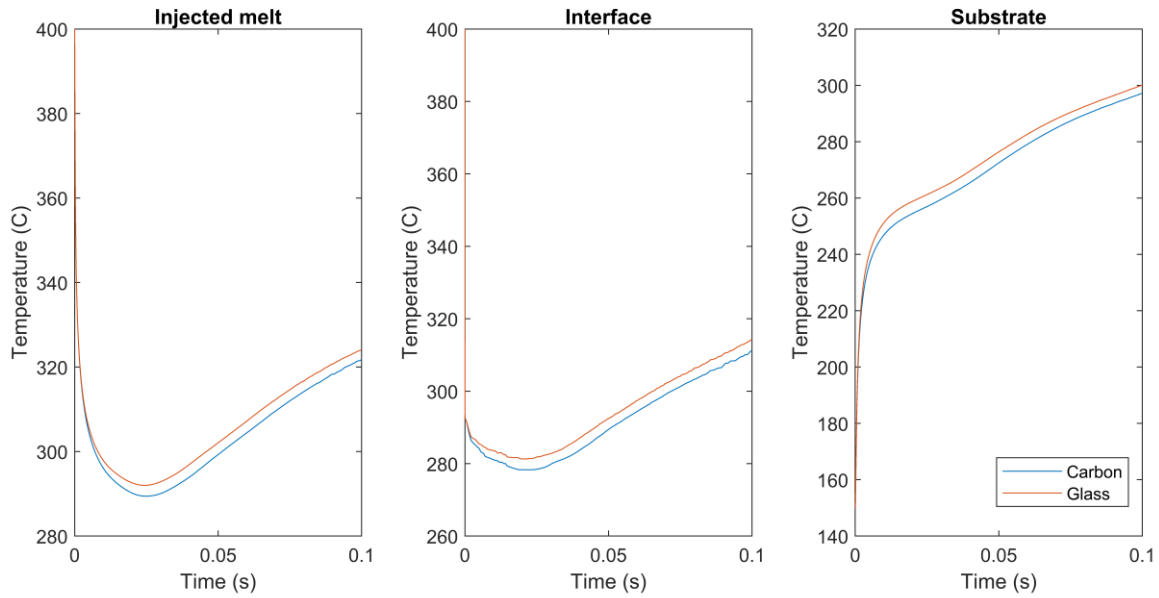


Figure 5: Comparison of thermal history for glass and carbon-loaded laminate geometry within proximity to the interface. The injected melt and substrate locations are recorded $10\mu\text{m}$ above and below the interface, respectively.

Mechanical testing of the lap-shear coupons revealed that the carbon-loaded samples consistently reported higher lap-shear strengths and lower deviation. From the inspection of the failure surfaces following testing, different failure mechanisms of the respective laminate systems are observed. At the interface of the carbon-reinforced system, the laminate remains intact, and polymer has been transferred between the surfaces, indicating that failure has occurred at the interface. On the fracture surface of the glass-reinforced laminate, there is evidence of fibres still bonded to the surface of the specimen, indicating that the capacity of the fibres to bear the load has been exceeded, resulting in the breakage of some of the fibres. The stochastic nature of the breakage of fibres in the system also offers a possible explanation for the considerably greater standard deviation of the glass fibre-reinforced system. Further investigation will be performed to isolate the interface strength and provide a definitive conclusion.

Sample	Average lap-shear strength (MPa)	Standard deviation (MPa)
<i>Carbon</i>	<i>15.46</i>	<i>0.33</i>
<i>Glass</i>	<i>13.90</i>	<i>1.01</i>

Table 1: Comparison of lap-shear strength of carbon and glass laminates.

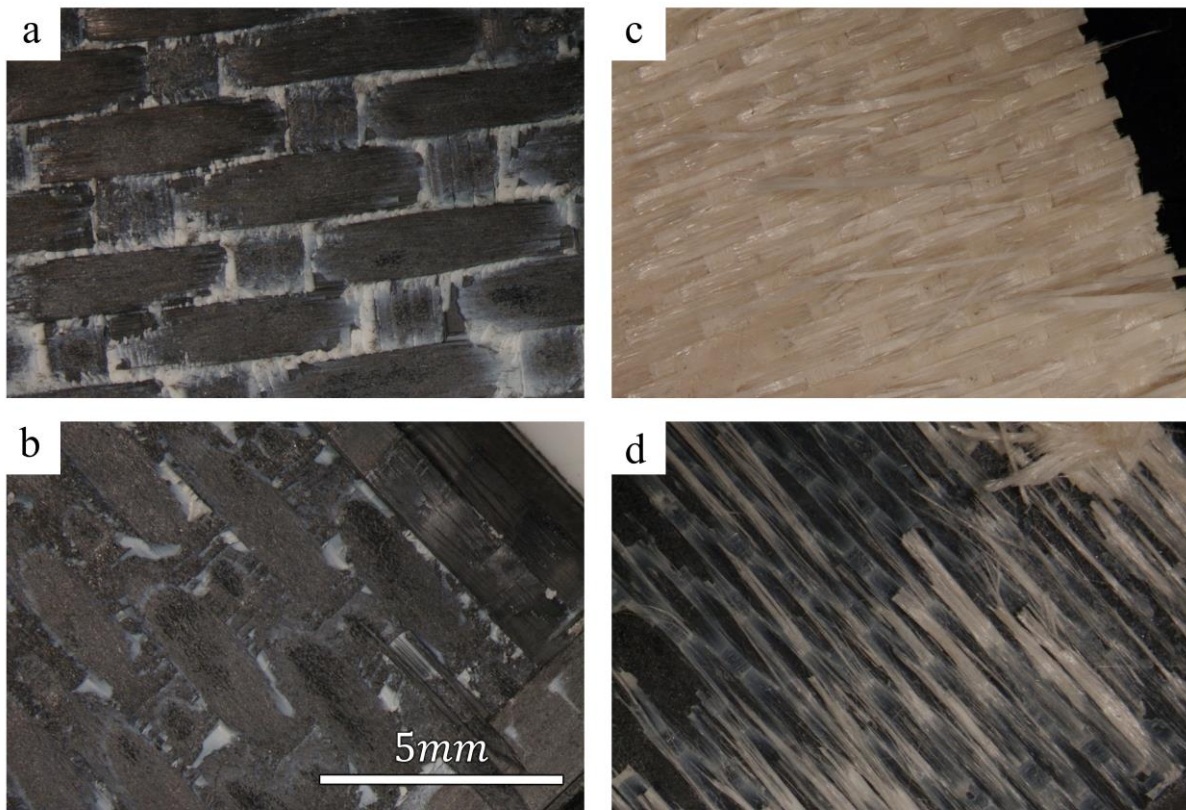


Figure 6: Failure surface following lap-shear test of overmoulded sample on the laminate and injected surfaces of the carbon-reinforced (a, b) and the glass-reinforced (c, d) laminates, respectively.

4 CONCLUSIONS

Interface morphology formation and strength have been investigated for composite injection overmoulded specimens with a focus on changing the substrate geometry and material. It is concluded from this investigation that despite an indication from the numerical simulation that a glass-reinforced substrate may provide preferable interface strength it is important to consider other factors in the ultimate strength of the composite structure. Understanding the interface strength is a multi-variable problem in which factors such as interface morphology, fibre architecture, thermal history as well as the material of the fibre reinforcement. Further work will be performed to further isolate the interface strength to provide a clearer conclusion on which fibre geometry provides improved interface strength.

ACKNOWLEDGEMENTS

I would like to gratefully acknowledge the Department for the Economy (DfE) for the funding of the project and Collins Aerospace UK for the provision of materials.

REFERENCES

- [1] M. Holmes, "Aerospace looks to composites for solutions," *Reinforced Plastics*, vol. 61, no. 4, pp. 237-241, 2017/07/01/ 2017, doi: <https://doi.org/10.1016/j.repl.2017.06.079>.
- [2] C. Hanser. (2013) From Laminate to Component. *Kunststoffe International*.
- [3] A. R. Carella, C. Alonso, J. C. Merino, and J. M. Pastor, "Sequential injection molding of thermoplastic polymers. Analysis of processing parameters for optimal bonding conditions," *Polymer Engineering and Science*, Article vol. 42, no. 11, pp. 2172-2181, 2002, doi: 10.1002/pen.11107.

- [4] A. Islam, H. N. Hansen, and M. Bondo, "Experimental investigation of the factors influencing the polymer–polymer bond strength during two-component injection moulding," *The International Journal of Advanced Manufacturing Technology*, vol. 50, no. 1-4, pp. 101-111, 2010.
- [5] R. Akkerman, M. Bouwman, and S. Wijskamp, "Analysis of the Thermoplastic Composite Overmolding Process: Interface Strength," (in English), *Frontiers in Materials*, Original Research vol. 7, no. 27, 2020-February-14 2020, doi: 10.3389/fmats.2020.00027.
- [6] A. Szuchács, T. Ageyeva, R. Boros, and J. G. Kovács, "Bonding strength calculation in multicomponent plastic processing technologies," *Materials and Manufacturing Processes*, vol. 37, no. 2, pp. 151-159, 2022/01/25 2022, doi: 10.1080/10426914.2021.1948052.
- [7] B.-A. Behrens *et al.*, "Numerical Modelling of Bond Strength in Overmoulded Thermoplastic Composites," *Journal of Composites Science*, vol. 5, no. 7, p. 164, 2021.
- [8] S. Wang, J. Shi, T. Shimizu, J. Xu, and Z. Xu, "Two-step heat fusion kinetics and mechanical performance of thermoplastic interfaces," *Scientific Reports*, vol. 12, no. 1, p. 5701, 2022/04/05 2022, doi: 10.1038/s41598-022-09573-3.
- [9] S. Adhikari, C. J. Durning, J. Fish, J.-W. Simon, and S. K. Kumar, "Modeling Thermal Welding of Semicrystalline Polymers," *Macromolecules*, vol. 55, no. 5, pp. 1719-1725, 2022/03/08 2022, doi: 10.1021/acs.macromol.1c02612.
- [10] G. A. Lyngdoh and S. Das, "Elucidating the Interfacial Bonding Behavior of Over-Molded Hybrid Fiber Reinforced Polymer Composites: Experiment and Multiscale Numerical Simulation," *ACS Applied Materials & Interfaces*, vol. 14, no. 38, pp. 43666-43680, 2022/09/28 2022, doi: 10.1021/acsami.2c09881.
- [11] M. A. Aravand and B. G. Falzon, "Characterisation of the interfacial bonding at solid/melt interfaces in multiphase carbon fibre reinforced thermoplastic composites," in *International Conference on Composite Materials (ICCM21)*, 2017.
- [12] M. A. Aravand, "Composite Injection Overmoulding," in *Design and Manufacture of Structural Composites*, L. Harper and C. M. Eds.: Woodhead Publishing, 2022.
- [13] J. Kattinger, T. Ebinger, R. Kurz, and C. Bonten, "Numerical simulation of the complex flow during material extrusion in fused filament fabrication," *Additive Manufacturing*, vol. 49, p. 102476, 2022/01/01/ 2022, doi: <https://doi.org/10.1016/j.addma.2021.102476>.